JOURNAL OF MATERIALS SCIENCE 25 (1990) 417–423

Deformation mechanisms in titanium dioxide single crystals

S TAKEUCHI, T. HASHIMOTO
Institute for Solid State Physics, University of Tokyo, Roppongi, Minato-ku, Tokyo 106, Japan

Single crystals of TiO_2 grown by a floating-zone method have been compressed in two directions, [1 0 0] and [0 0 1], at temperatures between 300 and 1300° C in an argon atmosphere. They deformed by $\{1\,0\,\bar{1}\}\langle 1\,0\,1\rangle$ slips, except [1 0 0] specimens tested below 600° C, where twinning preceded the slip deformation. Above 800° C, an oxygen reduction occurred during compression tests and the flow stress data were not reproducible. Below 700° C the data were reproducible and the resolved yield stress increased steeply with decreasing temperature. From the temperature and strain-rate dependences, activation analyses have successfully been performed. Activation volume becomes as small as $2b^3$ at high stress, and the deformation below 700° C is concluded to be governed by the Peierls mechanism. The total activation enthalpy of deformation by the Peierls mechanism is ~ 0.32 eV. Applying the string model for the kink-pair formation, the results are consistent if the $\langle 1\,0\,1\rangle$ dislocation is dissociated into two $\frac{1}{2}\langle 1\,0\,1\rangle$ partial dislocations. No twinning–anti-twinning asymmetry of slip was observed.

1. Introduction

As in the metal oxides with simple crystal structures, such as NaCl and wurtzite, single crystals of titanium dioxide with the tetragonal rutile structure are known to be easily deformable at high temperatures due to their rather simple crystal structure. Ashbee and Smallman [1, 2] investigated the active slip systems of this crystal by slip line observation and transmission electron microscopy, and found out that the primary slip system is the $\{1\,0\,\bar{1}\}\langle 1\,0\,1\rangle$ with a secondary system of $\{1\,1\,0\}[0\,0\,1]$. This observation was rather surprising because the h/b value for the $\{1\,0\,1\}\langle 1\,0\,1\rangle$ slip system is only the fourth largest value among those of the possible slip systems in the TiO_2 crystal, where h is the widest spacing of the lattice planes parallel to the slip plane and $\boldsymbol{b}$ the magnitude of the Burgers vector; the general trend is that the larger the h/b value the more active is the slip system. The h/b value for $\{1\,0\,\bar{1}\}\langle 1\,0\,1\rangle$ system is 0.177, while those for $\{1\,1\,0\}[0\,0\,1]$, $(0\,0\,1)\langle 1\,0\,0\rangle$ and $\{1\,0\,0\}[0\,0\,1]$ are 0.426, 0.322 and 0.301, respectively. Even if the anisotropic elasticity calculations are applied for the dislocation width parameter, ζ, which is the main factor determining the Peierls–Nabarro stress, the situation is the same [3]. Thus, the dissociation of a dislocation on the $\{1\,0\,\bar{1}\}\langle 1\,0\,1\rangle$ system into partial dislocations with the Burgers vector of $\frac{1}{2}\langle 1\,0\,1\rangle$ has been assumed in order to explain the experimental results [2, 3]. However, the weak-beam observation by transmission electron microscopy by Blanchin and Fontaine [4] has given no evidence of the dissociation, and also a high-resolution lattice image observation by Bursill and Blanchin [5] has shown that a dislocation is apparently undissociated in the bulk of the crystal.

It is known that the stoichiometric TiO_2 can be reduced to a lower oxygen concentration; in a low reduction range the induced defects are either titanium interstitials or oxygen vacancies and in the higher reduction range, crystallographic shear defects, well-known in this crystal [6], are introduced. The yield strength of the crystal has been shown to be sensitive to the deviation from the stoichiometry [2, 7], and it has been argued that the hardening due to the reduction is controlled by the interaction between the dislocations and the titanium interstitials [7]. It has also been shown that stoichiometric TiO_2 single crystals exhibit dynamic strain ageings at high temperatures [8].

The temperature regions of deformation experiments so far conducted have been limited mostly to a high-temperature range where the yield strength is determined by extrinsic defects and the deviation from stoichiometry, and no information has ever been obtained about the intrinsic strength of the crystal determined by the Peierls mechanism. The main purpose of the present paper is to analyse the intrinsic mechanical properties of TiO_2 by the use of high-quality single crystals of this material.

2. Experimental procedure

2.1. Single crystals

Single crystals of nearly stoichiometric TiO_2 have been produced in Chichibu Cement Co. Ltd by a floating zone (FZ) method in a lamp-image furnace [9]. The starting raw material was a commercial TiO_2 powder with purity better than 99.98%. A sintered rod with a diameter of about 14 mm, having a seed crystal with [0 0 1] axis, was zone-melted at a speed of 5 mm h^{-1}. The oxygen partial pressure of an inert gas atmosphere was less than 0.2%. The single crystals produced were about 10 mm diameter with a squarish

0022–2461/90 $03.00 + .12

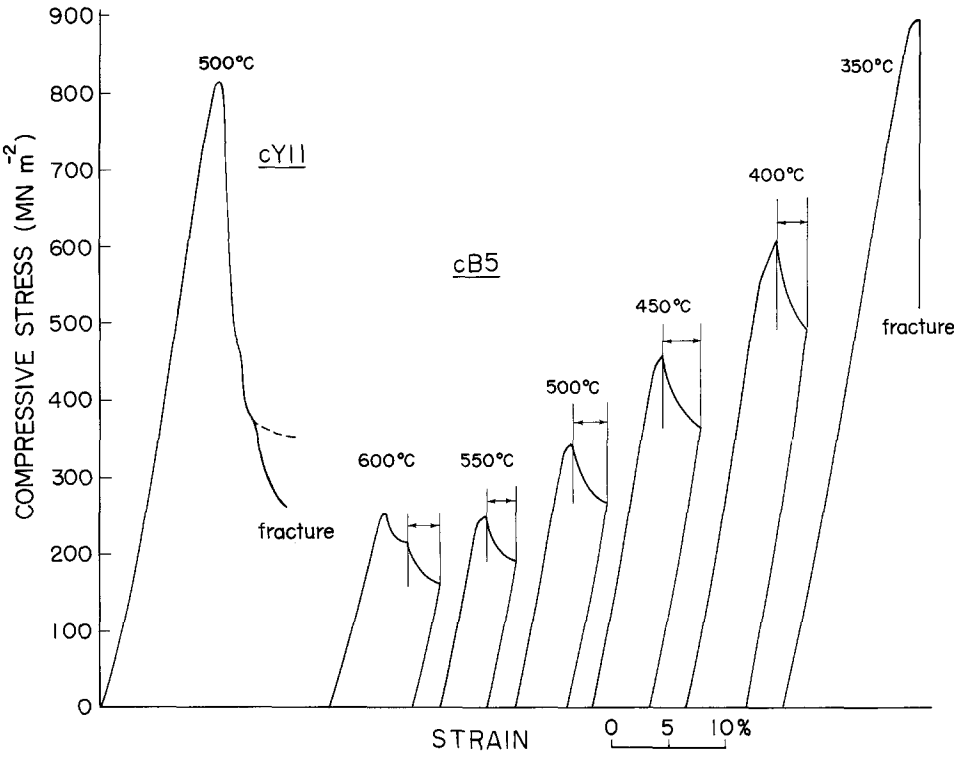

Figure 1 Compressive stress–strain curves for two [0 0 1] specimens, cY11 and cB5. The latter specimen was subjected to a successive temperature-change test. The regions indicated by horizontal arrows correspond to the stress relaxation curve.

cross-section having flat faces parallel to {1 1 0} planes. The as-grown single crystals were dark-bluish due to oxygen deficiency. After annealing in air at 850° C for 10 days, the crystals became yellowish and transparent. From the weight change measurements after annealing, the deviation from stoichiometry, x, in TiO_{2-x} in the as-grown crystal is estimated to be $x < 0.0005$, assuming that the annealed sample is stoichiometric.

The global crystal perfection of the single crystals was examined by a polarization microscope. From the birefringence contrast, existence of subgrains was detected. In the following experiments, we used two almost contrast-free single crystals of an as-grown crystal and an annealed crystal, which will be referred to as B and Y crystals, respectively. From the polarization microscope observations, it was found that these single crystals were of much better quality, with respect to the substructures, than any other available TiO_2 single crystals produced by the conventional Verneuil method.

2.2. Deformation experiments

Two types of rectangular compression specimens were cut from the Y and B crystals. One had the compression axis along the [0 0 1] direction with the side faces parallel to {1 1 0}, and the other had the compression axis along the [1 0 0] direction with the side faces parallel to (0 1 0) and (0 0 1). After cutting by a diamond wheel, the specimens were chemically polished in an aqueous solution of ammonium sulphate at 350° C. The size of the compression specimens was about $2.5 \times 2.5 \times 4\,mm^3$.

Compression tests were conducted in a tantalum-heater furnace in an argon atmosphere of 1 atm pressure. The strain-rate was $1.7 \times 10^{-4}\,sec^{-1}$. After yielding of a specimen at an initial deformation temperature, we obtained the stress relaxation curve by stopping the cross-head of the testing machine, unloading the specimen, changing the temperature by 50° C rise or fall, reloading the specimen, and repeating the same procedure. The amount of compressive strain at one temperature was 1% to 2%. By this series of experiments for each specimen, we obtained the temperature dependence of the initial flow stress from changes of the flow stress; in this procedure corrections of the stress were made by taking account of the work-hardening of the specimen at each temperature. In many cases, the direction of the temperature change was reversed after several steps to check the reproducibility of the stress. The results obtained indicated no appreciable difference between the Y and B samples. Therefore, no distinction will be made between the Y and B samples in the following descriptions.

The deformation markings on the surfaces of deformed specimens were observed by optical microscopy.

3. Results

3.1. [0 0 1] specimens

Fig. 1 shows stress–strain curves for two specimens. When the initial deformation temperature was below 550° C, the yield drop was so pronounced, as seen in specimen cY11 in the figure, that the specimen was fractured before the lower yield point was reached, or the upper yield stress was so high that fracture preceded yielding. Hence, the initial deformation temperature must be higher than 600° C to obtain temperature dependence of the flow stress and the strain-rate sensitivity. The flow stress increased rapidly with decreasing temperature below 600° C. When a specimen had been subjected to yielding at 600° C it could be

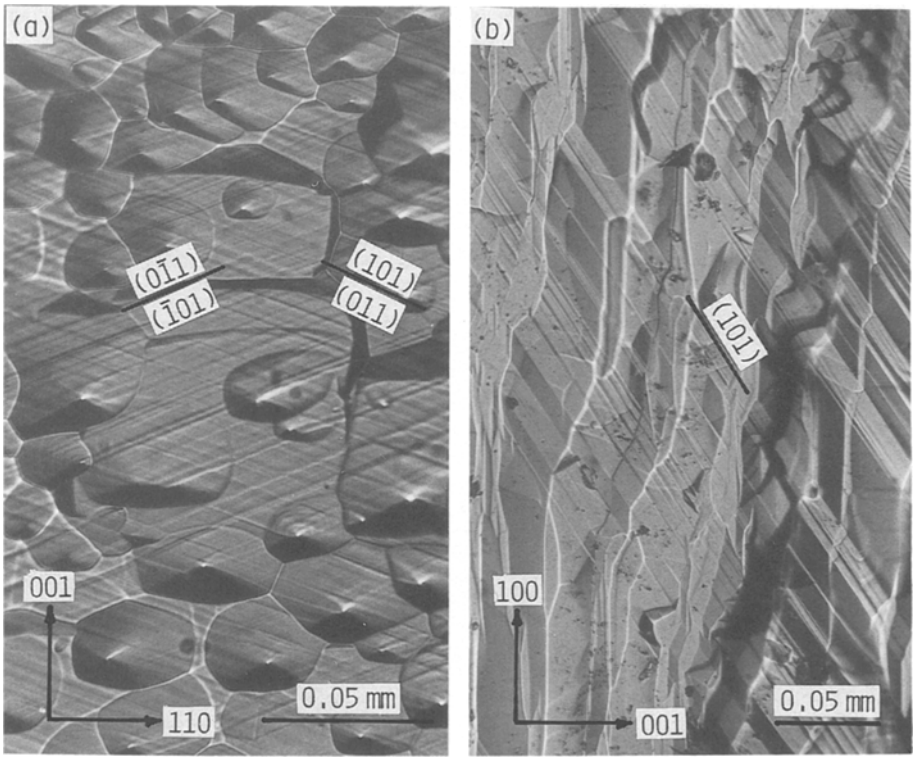

Figure 2 (a) Slip markings on a (1 1 0) face of a [0 0 1] specimen deformed between 550 and 800° C, indicating that $\{1\,0\,\bar{1}\}\langle 1\,0\,1\rangle$ slip systems have been activated. (b) The twinning deformation marks on the (0 1 0) plane of a [1 0 0] specimen. Vertical stripe patterns are due to surface contamination.

deformed down to a low temperature of 300 to 400° C without fracture, an example being given in Fig. 1 for specimen cB5. From the stress–relaxation curves, in the regions indicated by horizontal arrows in Fig. 1, the strain-rate sensitivity of the flow stress was estimated for each deformation temperature by measuring the stress decrement by which the slope of the relaxation curve changed by e^{-1}.

In the temperature change tests, when the deformation temperatures were below 700° C, the flow stress changes were almost reversible for the temperature reversal. However, above 800° C, when the temperature was reversed to a previous deformation temperature, the flow stress value, after correcting the work-hardening, always became higher than the previous one, indicating a compositional change during the high-temperature experiments in an argon atmosphere. In fact, after deformation at higher temperatures, the colour of the specimens changed to black, indicating an oxygen reduction; it is known that heating of TiO_2 single crystal in a non-oxidizing atmosphere causes oxygen reduction.

Fig. 2a shows the slip markings on a $\{1\,1\,0\}$ surface of a specimen deformed at temperatures between 800 and 550° C. The slip traces indicate that the activated slip systems were $\{1\,0\,\bar{1}\}\langle 1\,0\,1\rangle$ type consistent with the literature, and hence the compressive stress was resolved on this system in the following analyses.

Fig. 3 shows the temperature dependence of the resolved lower yield stress obtained from the temperature change tests, and the strain-rate sensitivity values obtained from the stress–relaxation curves. The order of the temperature change for each specimen is indicated by an arrow on the curve. The experimental values obtained for tests below 700° C almost fall on a single curve and are thus considered to be little affected by oxygen reduction. When the temperature was raised to higher temperatures above 800° C and then reversed, the flow stress value was always remarkably increased, and hence the data above 800° C have little meaning because they are for different compositions. Nevertheless, we observed a peak at around 1100° C in the stress–temperature curve as in previous works [2, 8], and also serrated flow in the same temperature range, indicating the dynamic strain ageing effect discussed in detail by Blanchin *et al.* [8].

3.2. [1 0 0] specimens

Fig. 4 shows the stress–strain curves for [1 0 0] specimens for the initial deformation temperatures below 600° C. Characteristic features are the serrated flow, which becomes less pronounced at lower temperatures, a weak temperature dependence of the flow stress and a much lower stress level compared with the flow stresses of [0 0 1] specimens in the same temperature range. Fig. 2b shows the deformation markings on the specimen aB9. Wide straight deformation bands are typical of the twinning deformation, of which the system is the same as the slip deformation, i.e. $\{1\,0\,\bar{1}\}\langle 1\,0\,1\rangle$. Fig. 5 shows plots of twinning stresses. In the case where a [1 0 0] specimen was first subjected to slip deformation at 700° C and then deformed at lower temperatures, the twinning did not take place even below 600° C, and the specimen could be deformed by slip down to 500° C. The suppression of the twinning deformation by pre-straining by slip is rather a common phenomenon in metallic crystals and is found to be the case also in this oxide crystal.

Fig. 6 shows an example of the irreversible temperature dependence of the flow stress for a [1 0 0] specimen. After heating the specimen up to 900° C, the flow stress at the initial deformation temperature of 700° C was remarkably increased, as in the case of [0 0 1] compression. Thus, the data above 800° C in Fig. 5 are again unreliable. However, between 1000 and 1200° C we observe two peaks, similar to those

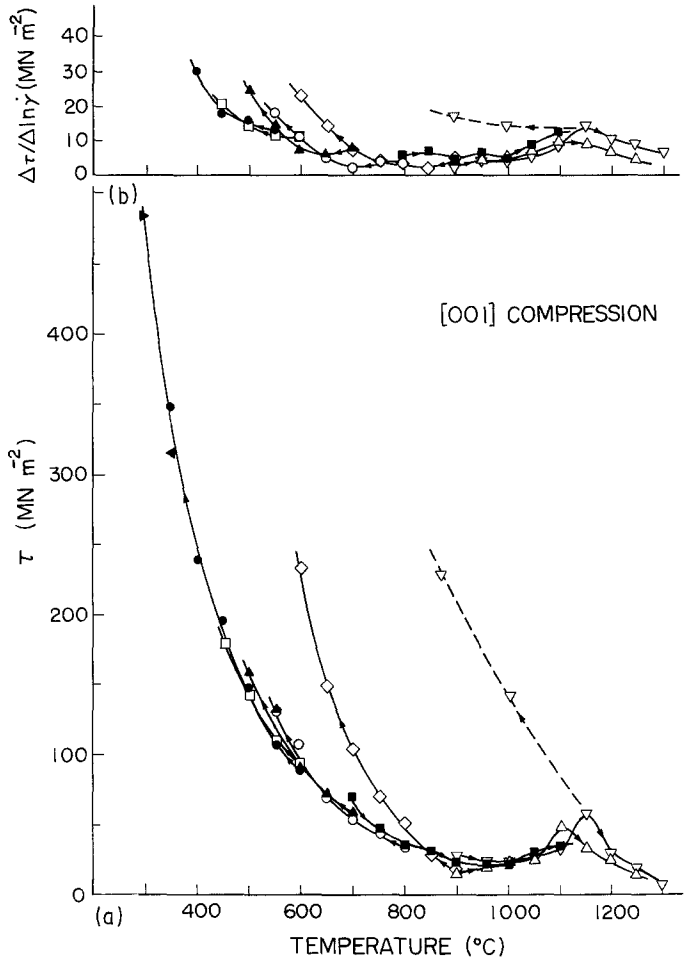

Figure 3 (a) The resolved yield stress plotted against temperature and (b) the strain-rate sensitivity data for [0 0 1] specimens. Similar symbols signify the same specimen. The direction of the temperature change is indicated by an arrow on each curve.

reported in stoichiometric single crystals by Blanchin *et al.* [8].

3.3. Activation analyses of deformation below 800° C

The shear strain rate of a crystal is generally expressed by an Arrhenius type equation given by

$$\dot{\gamma} = \dot{\gamma}_0 \exp\left(-\frac{\Delta H(\tau^*)}{k_B T}\right) \quad (1)$$

where $\dot{\gamma}_0$ is the prefactor, ΔH is the activation enthalpy of deformation as a function of the effective stress τ^* and $k_B T$ have the usual meanings. The activation volume defined by $v^*(\tau^*) = -\mathrm{d}\Delta H/\mathrm{d}\tau^*$ has been obtained from the strain-rate sensitivity data according to the relation

$$v^*(\tau^*) = k_B T\left(\frac{\partial \ln \dot{\gamma}}{\delta \tau^*}\right)_T \quad (2)$$

The activation enthalpy can also be obtained from the strain-rate sensitivity and the temperature dependence of the flow stress by the relation

$$\Delta H(\tau^*) = -k_B T^2\left(\frac{\partial \dot{\gamma}}{\partial \tau^*}\right)_T\left(\frac{\partial \tau^*}{\partial T}\right)_{\dot{\gamma}} \quad (3)$$

The validity of the Arrhenius relation can be checked by the constancy of the $\Delta H/(k_B T)$ values experimentally obtained for a constant strain rate.

The resolved yield stresses and the strain-rate sensitivities below 800° C exhibit no essential differences between [0 0 1] and [1 0 0] specimens, and between Y and B samples, as presented in Figs 3 and 5. The activation volumes and the activation enthalpies have been calculated by using the strain-rate sensitivity data and the slope of the τ–T curves in Figs 3 and 5. The results are plotted in Fig. 7. Here, τ^* values are the resolved shear stresses subtracted commonly by the athermal stress of 25 MN m^{-2}, which is the approximate leveling-off value above 800° C, and $\boldsymbol{b}$ is the magnitude of the Burgers vector of the $\langle 1\,0\,1\rangle$ dislocation. Owing to the uncertainties of the experimental data, the calculated values are largely ambiguous. Nevertheless, as shown in Fig. 8, the $\Delta H/(k_B T)$ values for a constant strain rate are almost constant around 30 to 40. Thus, the results of Fig. 7 are valid approximately.

4. Discussion

The growth process, an FZ method, of the present

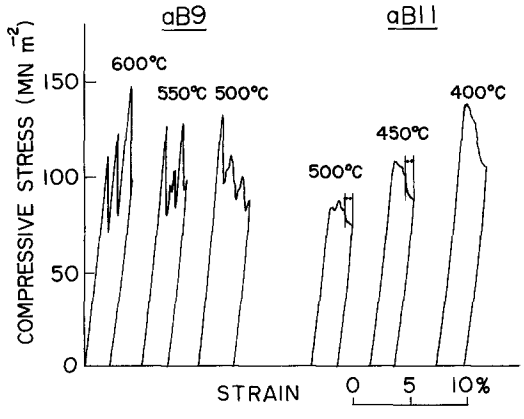

Figure 4 Twinning deformation curves for two [1 0 0] specimens.

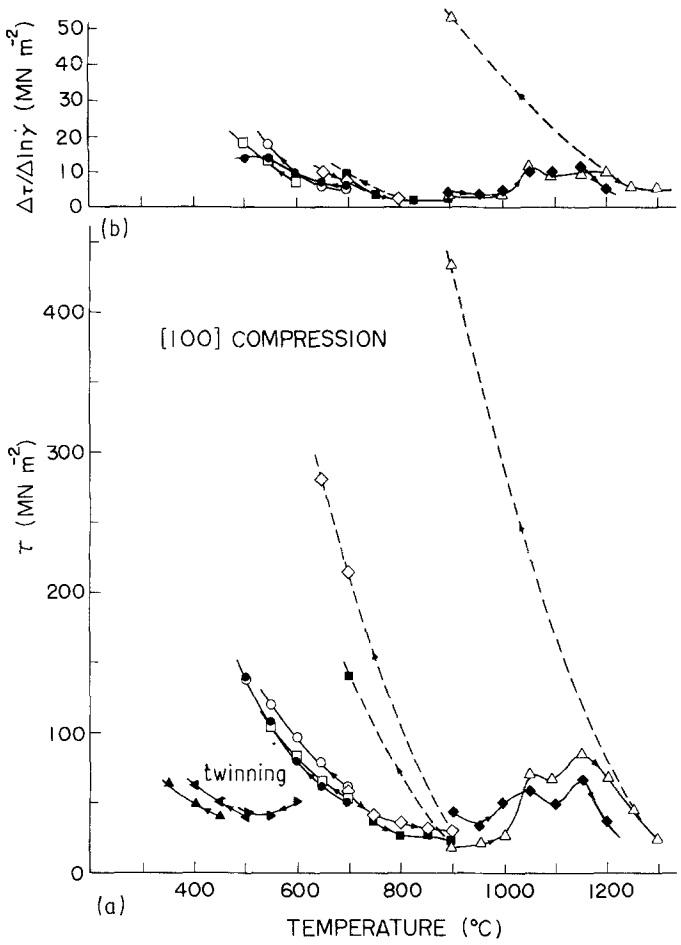

Figure 5 (a) The resolved yield stress–temperature curve and (b) the strain-rate sensitivity data for [1 0 0] specimens. (▲) Twinning stresses.

crystals, is different from that of the crystals used previously for deformation experiments, i.e. the Verneuil method. We observed, however, no essential difference in the flow stresses between the present data and the previous data. The only difference, if any, may be in that the present crystals are less brittle than the previous ones, because they could be deformed down to lower temperatures than the previous experiments. This fact may possibly be due to a much lower density of subboundaries in the present crystals.

The results below 800° C for Y and B samples indicate that the flow stress in this temperature region is not sensitive to the slight deviation from stoichiometry. From the fact that the activation volume becomes as small as a few b^3 as the temperature is lowered, the deformation below 700°C in both samples is considered to be controlled by the Peierls mechanism.

The theory of the Peierls mechanism based on the string model of the dislocation [10] leads to the following relationship between the total activation enthalpy, ΔH_0, and the Peierls stress, τ_p [11]

$$\frac{H_0}{Kb^3} = (1.0 \pm 0.3)\left(\frac{d}{b}\right)^{3/2}\left(\frac{\tau_p}{K}\right)^{1/2} \quad (4)$$

where d is the spacing between the Peierls valleys, K

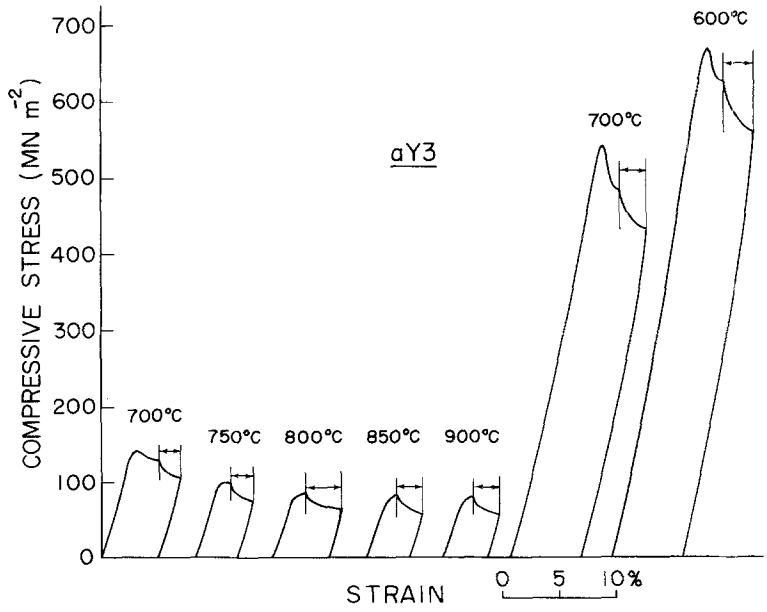

Figure 6 A series of compression stress–strain curves for a [1 0 0] specimen. The stress-relaxation regions are indicated by horizontal arrows.

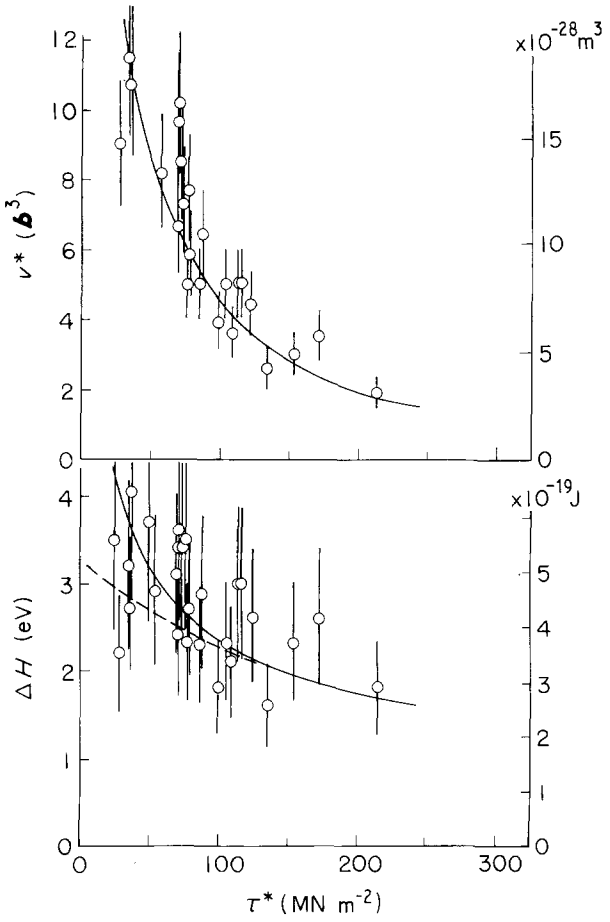

Figure 7 Activation volume, v^*, and activation enthalpy, ΔH, as a function of effective stress, τ^*, which is the resolved yield stress subtracted by the athermal stress 25 MN m^{-2}.

the line tension factor of the dislocation. Assuming that the edge dislocation controls the deformation as suggested by the TEM observation [8], the d = 0.272 nm and the K is calculated to be 122 GN m^{-2} [3]. Using the experimental value of $\Delta H_0 \simeq 3.2$ eV, the τ_p value calculated according to Equation 4 is 0.4 to 1.3 GN m^{-2} for b = 0.5465 nm (perfect dislocation) and 3 to 10 GN m^{-2} for b = 0.273 nm (partial dislocation).

The most reliable estimation of the Peierls stress is to extrapolate the τ–T relation to the absolute zero temperature. Practically, however, this procedure is generally difficult because of the brittle fracture of the crystals at low temperatures. The same is true for the present case. However, it seems safe to state from the τ–T relation in Fig. 3, that the extrapolated stress at absolute temperature is much higher than 1 GN m^{-2}. Thus, the above estimation of τ_p based on Equation 4 for the perfect dislocation is obviously not consistent with the experiment, whereas the τ_p value estimated for the partial dislocation seems reasonable.

It has been demonstrated previously [11] that the experimentally estimated Peierls stresses are in order-of-magnitude agreement with the Peierls–Nabarro expression of the Peierls stress, i.e.

$$\tau_p = G/(1 - \nu) \exp [-2\pi/(1 - \nu)h/b] \quad (5)$$

where G is the shear modulus and ν the Poisson ratio [12]. For the perfect and partial dislocations in the present crystal, the calculated values are τ_p = 50 GN m^{-2} and 10 GN m^{-2}, respectively. The latter value is consistent with the τ_p value estimated from Equation 4, while the former value is not.

Thus, the experiments and the theoretical relations for the Peierls mechanism are consistent if the [1 0 1] dislocations are dissociated into partial dislocations, and not consistent if undissociated. Although the TEM experiments so far performed have not supported the dissociation as mentioned previously, such experiments have been quite limited and might not have provided us with the general information, especially about mobile dislocations. More high-resolution electron microscopy experiments seem necessary to reveal the structure of {1 0 1}, ⟨1 0 1⟩ glide dislocations.

Because of the tetragonality of the crystal, the (1 0 $\bar{1}$)[1 0 1] and the (1 0 $\bar{1}$)[$\bar{1}$ 0 $\bar{1}$] shear are not equivalent to each other; the former is the twinning shear and the latter the anti-twinning shear. The [1 0 0] compression corresponds to the former and the [0 0 1] comporession to the latter. It may be expected that the Peierls stresses for these two opposite shears are different from each other, like the well-known {1 1 2} slip asymmetry in bcc metals. However, comparing the τ–T curves in Figs 3 and 5, we cannot detect any difference in the flow stress for the two different shears in the tested temperature range.

Possible atomic configurations of a $\frac{1}{2}$⟨1 0 1⟩{1 0 $\bar{1}$} stacking fault and a twin boundary are drawn in Fig. 9. In the original dissociation model by Ashbee and

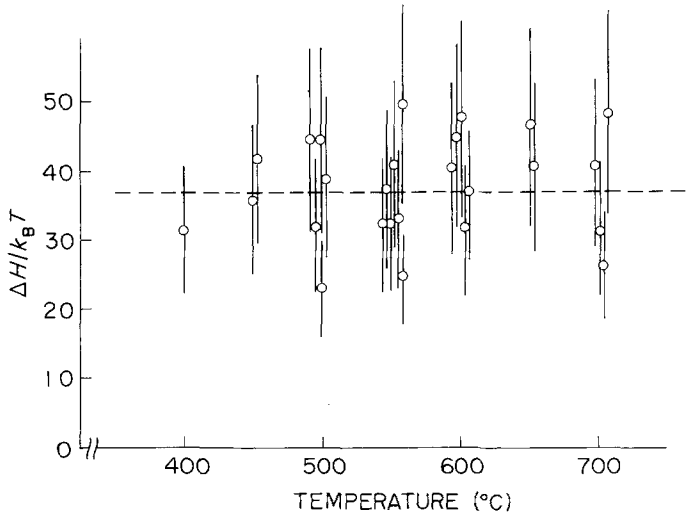

Figure 8 $\Delta H/(k_B T)$ values at various temperatures for a constant strain rate ($\dot{\gamma} \simeq 2 \times 10^{-4}$ sec^{-1}).

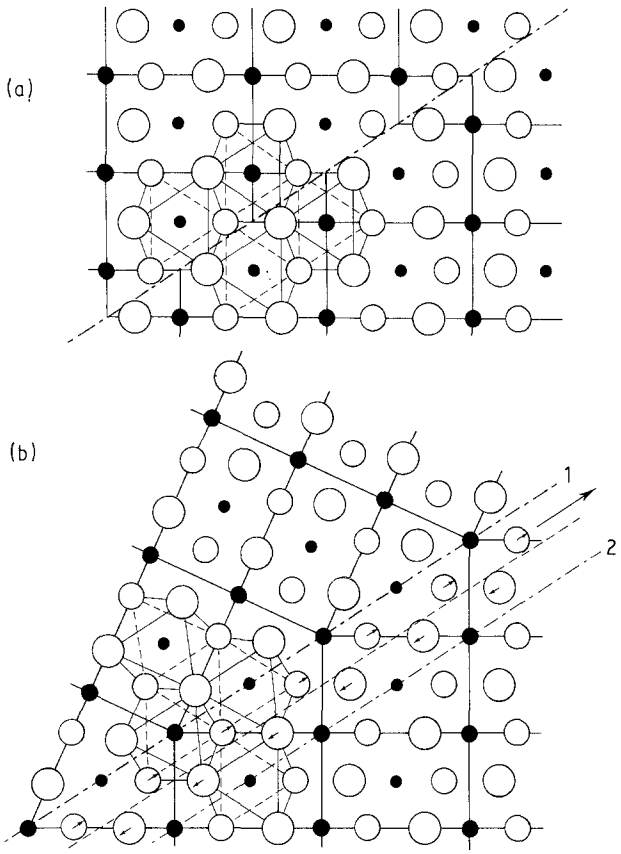

Figure 9 (a) A possible atomic configuration at a $\frac{1}{2}(1\,0\,\bar{1})[1\,0\,1]$ stacking fault viewed from the [0 1 0] direction. (○) Oxygen atoms, (●) titanium atoms. Some octagonal oxygen cages are shown. (b) A possible atomic configuration at a $\{1\,0\,\bar{1}\}$ twin boundary. Shufflings of the oxygen atoms accompanying the movement of the boundary from position 1 to position 2 by a passage of a twinning dislocation are shown by small arrows.

Smallman [2], the fault plane was assumed to lie in between an oxygen layer and a titanium layer, but in Fig. 9a the fault plane is assumed in between two adjacent oxygen layers, because the lattice spacing of the latter is wider than the former. As seen in the figure, the octagonal oxygen cages around titanium atoms are almost preserved in the fault plane and hence the fault seems to have a low energy.

As seen in Fig. 9b, the atomic configuration in the twin boundary plane is similar to the stacking fault plane, though the octagonal oxygen cage at the boundary is slightly distorted. For the thickening of the twin, a twinning dislocation, whose Burgers vector is shown by a large arrow in Fig. 9b, glides between two adjacent oxygen layers (shown by a dashed line) with slight shufflings of the oxygen atoms in these layers shown by small arrows, and thus the boundary plane moves from plane 1 to plane 2 in the figure. The magnitude of the Burgers vector of the twinning dislocation, $(a^2 - c^2)/(a^2 + c^2)^{1/2} = 0.226\,\text{nm}$, is about 83% of the $\frac{1}{2}[1\,0\,1]$ partial dislocation. Owing to this smaller Burgers vector of the twinning dislocation, the Peierls potential must be lower than that of the partial dislocation. This may be the reason why the twinning shear stress is lower than the resolved shear stress for slip.

Acknowledgements

The high-quality TiO_2 single crystals were produced by Dr A. Asaumi and Mr K. Shimizu, Chichibu Cement Co. Ltd. The authors are indebted to them for supplying the single crystals for the present experiment.

References

1. K. H. G. ASHBEE and R. E. SMALLMAN, *J. Amer. Ceram. Soc.* **46** (1963) 211.
2. K. H. G. ASHBEE and R. E. SMALLMAN, *Proc. Roy. Soc. London* **A274** (1963) 195.
3. Y. MOTOHASHI, M. G. BLANCHIN, E. VICARIO, G. FONTAINE and S. OTAKE, *Phys. Status Solidi (a)* **54** (1979) 355.
4. M. G. BLANCHIN and G. FONTAINE, *ibid.* **29** (1975) 491.
5. L. A. BURSILL and M. G. BLANCHIN, *Phil. Mag.* **A49** (1984) 365.
6. L. A. BURSILL and B. G. HYDE, in "Progress in Solid State Chemistry", Vol. 7, edited by H. Reiss and J. O. McCaldin (Pergamon Press, Oxford, 1972) p. 177.
7. M. VRINAT and M. G. BLANCHIN, *J. de Phys.* **42** (1981) C3-77.
8. M. G. BLANCHIN, G. FONTAINE and L. P. KUBIN, *Phil. Mag.* **A41** (1980) 261.
9. M. HIGUCHI, T. HOSOKAWA, K. SHIMIZU, S. KIMURA, K. KITAMURA and N. II, *J. Jpn Assoc. Crystal Growth* **13** (1986) 83 (in Japanese).
10. J. E. DORN and S. RAJNAK, *Trans. Met. Soc. AIME* **230** (1964) 1052.
11. S. TAKEUCHI and T. SUZUKI, in "Strength of Metals and Alloys", edited by P. O. Kettunen, T. K. Lepisto and M. E. Lehtonen (Pergamon, Oxford, 1988) p. 161.
12. F. R. N. NABARRO, "Theory of Dislocations" (Oxford University Press, 1967) pp. 175–88.

Received 28 October 1988
and accepted 14 April 1989